Published in final edited form as:
Analyst. 2013 June 7; 138(11): 3126–3130. doi:10.1039/c3an00093a.

Sonophoric nanoprobe aided pH measurement *in vivo* using photoacoustic spectroscopy†

Aniruddha Ray[a,b], **Hyung Ki Yoon**[b], **Yong Eun Koo Lee**[b], **Raoul Kopelman**[a,b], and **Xueding Wang**[c]

Raoul Kopelman: kopelman@umich.edu; Xueding Wang: xdwang@umich.edu

[a]Biophysics, University of Michigan, Ann Arbor, MI, USA

[b]Department of Chemistry, University of Michigan, Ann Arbor, MI, USA

[c]Department of Radiology, University of Michigan, Ann Arbor, USA

Abstract

Presented here is a novel method of *in vivo* pH sensing utilizing a hybrid optical imaging technique, photoacoustic imaging (PAI), and pH sensitive polymeric nanoprobes. Nanoprobes with hydrophobic core containing a pH sensitive dye were synthesized and used to measure the pH level *ex vivo* first and then *in vivo* by performing experiments on a rat joint model, with an achieved precision of less than 0.1 pH units. The ability of the hydrophobic functional groups in the polyacrylamide matrix to shield the molecular dye from being affected by the proteins in the plasma, and prevent the dye from leaching out, is also demonstrated.

Introduction

The pH level is one of the most important parameters in many physiological, pathological and therapeutic processes. Since pH is strictly regulated, abnormal pH levels can act as indicators for diseases or other bodily dysfunction. Deviations in pH may reflect body stress conditions such as inflammation, high exercise levels, interruption of normal blood supply, and biochemical shock. According to previous studies,[1] a lower pH level is a typical characteristic of cancerous tissues, which also affects the delivery and effectiveness of drugs to the tumor.[2] Other clinical examples of anomalous tissue pH include arthritis[3] and wounds.[4] Thus monitoring the pH at tissue and intracellular level *in vivo* could help diagnose the severity of diseases and monitor disease progression, as well as treatment progression.

Several methods, including positron emission tomography (PET),[1,5] magnetic resonance spectroscopy (MRS) and imaging (MRI)[1,6] have been utilized previously for measuring the pH of tissues *in vivo*. Although they are very widely used, these methods have their own disadvantages such as high cost, low sensitivity and low temporal resolution. Additionally PET utilizes ionizing radiation which also limits its usage. Optical methods provide an

†Electronic supplementary information (ESI) available. See DOI: 10.1039/c3an00093a

Correspondence to: Raoul Kopelman, kopelman@umich.edu; Xueding Wang, xdwang@umich.edu.

alternate and attractive solution due to their low cost, non-invasiveness, utilization of non-ionizing radiation and ability of continuous online monitoring of the dynamic pH changes. The optical pH measurements are generally performed using exogenous contrast agents such as pH sensitive dyes, polymers or nanoprobes, by an intensity-based, ratiometric fluorescence excitation or emission method[7,8] or by the fluorescence lifetime method.[9] However, due to the strong scattering of light in most biological tissues, conventional optical techniques such as fluorescence imaging, have limited spatial resolution and penetration depth when working in a light diffusion regime. Combining the advantages of light and ultrasound, the emerging biomedical photo-acoustic technique has the ability to overcome the above mentioned drawbacks and has been extensively utilized for both imaging and sensing applications.[10,11] As an example, the feasibility of the photoacoustic technique for pH sensing and imaging has been previously demonstrated *in vitro*.[12-14] These previous studies used the techniques of photoacoustic spectroscopy and microscopy, to demonstrate the feasibility of functional imaging, but were limited to demonstrations on tissue phantoms. The molecular contrast agents used in previous studies, however, are not suitable for *in vivo* applications.

Here we demonstrate, for the first time, a ratiometric photoacoustic based method for *in vivo* pH sensing using pH sensitive nanoprobes. The nanoprobes consist of the pH sensitive dye seminaphthorhodafluor (SNARF-5F) encapsulated in a polyacrylamide hydrogel matrix. SNARF-5F has a pK_a value of 7.2, making it ideal for pH measurements in the physiologically relevant range. The nanoprobes have a relatively hydrophobic core, so as to efficiently trap the SNARF-5F molecules inside. The polyacrylamide matrix protects the dye from interacting with the external proteins and cell organelles in the plasma, but allows free flow of ions and small molecules, such as O_2, through the matrix. As demonstrated in previous studies, the interaction of the pH sensitive dyes with different proteins often leads to an undesirable change in the optical properties of those dyes.[15] Therefore, by using the nanoprobe design, the optical and chemical properties of the pH sensitive dyes are better preserved in the complex *in vivo* environment, which is essential to achieve a quantitative evaluation of pH levels inside live biological samples. The polyacrylamide matrix of the nanoprobes is biocompatible, biodegradable, and can be retained in the cytoplasm for days. Moreover, by surface modification and attachment of different peptides or antibodies, the nanoprobes can be targeted to specific cells or tissues.[16] This nanoparticle platform enables specifically targeted delivery of the unmodified SNARF dye. For specific targeting applications, the SNARF dye itself can also be modified to have different functional group as well, which can be used for attachment to targeting peptides or antibodies. However the SNARF dye with an attached functional group is significantly more expensive than the dye without the functional group. Furthermore, the direct attachment of the peptides to the dye often leads to unwanted changes in its optical characteristics and physical properties.[17]

Experimental

The nanoprobes were prepared using a reverse micelle poly-merization process as shown in ESI, Fig. 1.[†18] The monomers acrylamide (689.5 mg, 97%), 3-

[†]Electronic supplementary information (ESI) available. See DOI: 10.1039/c3an00093a

(aminopropyl)methacrylamide hydrochloride salt (APMA), the hydrophobic crosslinker (53.6 mg, 3%), glycerol dimethacrylate (GDMA) (480 μL, 20%), and the dye SNARF (3 mg) (Invitrogen, Carlsbad, CA) are added and emulsified in a surfactant solution of AOT (1.6 g) and Brij-30 (3.3 mL) in Hexane (45 mL), before initiating the reaction using *N*,*N*,*N*′,*N*′-tetramethylethylenediamine (TEMED) (100 μL) and 10% (w/w) ammonium persulfate (APS) (100 μL). The reaction is allowed to continue for two hours and then hexane is removed by rotary evaporation, before washing the particles in ethanol and water several times in an amicon filter cell, with 300 kDa membrane, so as to remove the surfactants and any unreacted monomer. Acrylamide, methylene-bis-acrylamide (MBA), glycerol dimethacrylate (GDMA), dioctyl sulfouccinate (AOT), Brij 30, hexane, ammonium persulfate (APS), *N*,*N*,*N*′,*N*′-tetramethyl ethylenediamine (TEMED), 3-(aminopropyl)methacrylamide hydrochloride salt (APMA) was obtained from Polysciences Inc. (Warrington, PA).

Result and discussion

The average hydrodynamic size of the nanoprobes in aqueous medium was obtained by monitoring the dynamic light scattering and was measured to be 53 nm, with a polydispersity index of 0.19. They also had a surface charge of +18 mV, making them very suitable for cellular uptake. The amount of dye encapsulated in the nanoprobes was estimated by comparing the fluorescence from a known concentration of nanoprobes and the fluorescence calibration curve of free dye. We estimate that the nanoprobes encapsulate about 0.3% of the dye by weight. This result was further confirmed by comparing absorbance measurements from the dye and the absorption calibration curve. Due to the nonpolar nature of the dye, it was not possible to achieve higher dye loading into the matrix. However, the dye loading efficiency can be improved by conjugating the dye to the nanoparticle matrix by special functionalization of the dye. Encapsulation of the dye inside the nanoparticle results in a red shift in the absorption spectrum of the dye (compared to free dye), due to interaction with the matrix, as shown in ESI, Fig. 2.† In addition to that we also observe a reduction in the sensitivity of the dye to pH, when present inside the matrix, compared to “free” dye. However, as the important properties of the dye, such as its extinction coeficient, remain unperturbed, the nanoprobes can serve as reliable pH sensors, after calibration in buffers, and their properties are preserved both *in vitro* and *in vivo*. The presence of the hydrophobic functional group in GDMA and APMA makes the core hydrophobic, thus helps encapsulate the SNARF dye efficiently. For nanoprobes without GDMA, containing *N*,*N*′-methylenebisacrylamide, and lower amount of APMA, the amount of dye encapsulated inside the matrix was significantly lower (<5×). The dye leaching from the nanoprobes was tested in PBS and we did not observe any dye leaching even after 24 hours.

To demonstrate the effectiveness of the nanoprobe matrix for protecting the encapsulated dye, we studied the interaction of the SNARF free dye *versus* that of the nanoprobes containing the SNARF dye with albumin, a protein most abundantly presents in the blood and tissues. This was done by monitoring the absorbance, of the free dye and of the nanoparticles, at a dye concentration of 3 μg mL^{-1}, using a spectrophotometer [Shimadzu UV-Vis 1601]. We observed that the free dye, on interaction with albumin, partially lost its

color instantly. Its absorbance throughout the spectrum, from 500 nm to 600 nm, was reduced by almost 90% from the initial value, as shown in Fig. 1. In comparison, the SNARF dye encapsulated in the nanoprobe matrix was much better protected from the effect of albumin. A mild loss of less than 20% in absorbance was observed, even after 48 hours of incubation. The long term stability of the dye inside the nanoprobes demonstrates good encapsulation, *i.e.*, it benefited from the hydrophobic functional groups in the nanoprobes, which successfully prevented the dye from leaching out in the presence of albumin.

The setup for spectroscopic photoacoustic measurement of pH level on live rats is shown in Fig. 2. A tunable dye laser (ND6000, Continuum) pumped by the second harmonic of a pulsed Nd:YAG laser (Powerlite, Continuum) was used to provide pulsed light with a pulse width of 5 ns and pulse repetition rate of 10 Hz. The two wavelengths used for spectroscopic measurement were 565 nm and 580 nm. Light fluence of about 5.1 mJ cm^{-2} at 580 nm, and of 3.8 mJ cm^{-2} at 565 nm was used to generate photoacoustic signals. These light fluence are much lower than the ANSI safety limit for human skin. We do not use any reference channel since the dye laser is very stable, with a pulse to pulse fluctuation <5%. This pulse to pulse fluctuation is averaged out by taking the average over 30 pulses. Before *in vivo* experiments on live rats, we first acquired a pH calibration curve through the *in vitro* experiment on phantoms. The nanoprobes containing the pH sensitive dye was injected, using a syringe pump, into a section of transparent soft tubing (0.58 mm BD Intramedic, Sparks, MD, USA) mimicking a blood vessel. The photoacoustic signal created from the nanoprobes in the tubing was detected by a high-sensitivity and wide-bandwidth (132.63% at −6 dB with a center frequency of 9.01 MHz) ultrasonic transducer (V312, Panametrics). The transducer was cylindrically focused on the tubing with a focal length of 0.75 inch. The signals received by the transducer were amplified and digitized by a 500 MHz digital oscilloscope (TDS 540B, Tektronix) before being transferred to a computer. For each data point, the signal averaging was performed over 30 measurements to improve the signal-to-noise ratio. As shown in Fig. 3, the ratio between the photoacoustic signal intensities at the two wavelengths, *i.e.* 580 nm and 565 nm, increases linearly in the pH range from 6.0 to 8.0. The ratio was calculated using the following equation:

$$Ratio = \frac{I_{580nm}^{postinjection} - I_{580nm}^{preinjection}}{I_{565nm}^{postinjection} - I_{565nm}^{preinjection}} = Const \times pH$$

The constant factor, which can be obtained from the slope, determines the sensitivity of the probe. The pH response of the dye is sigmoidal in nature, as governed by the Henderson–Hasselbalch equation. The linear region of the sigmoidal curve is determined by the pK_a of the dye. For SNARF 5F the pK_a value is 7.2. Therefore, we perform the calibration over the pH region 6–8, which is also the physiologically most relevant range.

To examine whether photoacoustic measurement of pH level can be achieved in an *in vivo* environment, experiments were performed on a rat joint model (Sprague Dawley, 100 g body weight, Charles River Laboratory). During the whole experiment, the rats were anesthetized using isoflurane. To prevent motion, the rat was placed on a pad and its tail was fixed firmly on a 45° inclined platform. Both the rat tail and the transducer were placed in

water for ultrasound coupling. The nanoprobes (200 μL) containing the pH sensitive dye were injected locally into a tail joint. The center of the joint space was 2–3 mm deep from the skin surface of the tail. Before injection, the nanoprobe solutions were prepared by suspending them in deionized water (pH 7) and pH buffer (pH 8) respectively, leading to a dye concentration of 300 microgram per mL. The spectroscopic photoacoustic measurement of the pH level in the target tail joint was conducted by illuminating the collimated light beam, at 580 nm and 565 nm wavelengths respectively, on the surface of the tail and pointing the ultrasonic transducer to the illuminated area. Then photoacoustic signals, correspondent to the two wavelengths, were recorded from the joint area, an example shown in Fig. 4. By subtracting the signal before nanoprobe injection from the signal after injection, the background photoacoustic signal was removed. This change in photoacoustic signal after injection is directly proportional to the absorption of the dye. The local pH level in the joint was then determined by comparing the ratio of the photoacoustic signal intensities at the two wavelengths with the *in vitro* calibration curve in Fig. 3. Before computing the ratio, the difference in tissue optical attenuation between the two wavelengths was also compensated using the tissue optical parameters from the literature.[19] The average pH levels were 7.1 ± 0.1 in the tail joints with injected nanoprobe solution in de-ionized water (pH 7); while the average pH levels were 7.8 ± 0.1 in the tailed joints with injected nanoprobe solution in pH buffer (pH 8), both close to the respective preset pH level of the solution. The small deviation between photoacoustic measurements and the preset values may be attributed partially to the mixing of the nanoprobe solution with the joint fluid.

This system is capable of acquiring data at a frequency of 10 Hz, limited only by the pulse repetition rate of the pump laser. For the current study we used a single transducer. However an ultimate clinical device for functional imaging would involve a transducer array. Such type of system could easily be automated, and it would be possible to obtain a complete tissue pH mapping within seconds, making it into a rapid imaging and sensing device. However for intravenous injection, the time limiting step will be the injection of the nanoprobes and their accumulation time in the target tissue. Compared to free dye molecules, which generally have a short blood circulation lifetime ($\tau_{1/2}$ ~ order of minutes), these nanoprobes have a much longer circulation lifetime ($\tau_{1/2}$ ~ hours), depending on the surface functionality, such as polyethylene glycol (PEG), cell specific antibodies or peptides. The attachment of PEG and targeting moieties onto the nano-particles not only increases the circulation time, as it helps evade uptake by macrophages, but also achieves specificity towards the target tissue. The current limit for PAI detection is 0.10 mM dye. Even with intravenous injection, it would be possible to achieve this concentration threshold at the target tissue when using specific targeting moieties, as has been demonstrated previously for other applications.[16] However the threshold concentration will depend on the application and the depth of measurement.

Conclusion

We demonstrate, for the first time, through experiments on phantoms and live animals, the feasibility of quantifying pH level using ratiometric intensity based spectroscopic photoacoustic measurement facilitated with pH sensing nanorpobes. Our results show that the properties of the dye in its free form get severely altered in the presence of albumin. In

comparison, the nanoprobes, consisting of polyacrylamide matrix with a hydrophobic core, largely prevent the interaction of the dye with proteins appearing prevalently in the *in vivo* environments. We observed a 90% reduction in the absorbance of free dye in the presence of albumin, compared to only a 20% reduction for the nanoprobes. Preserving the optical properties of the pH sensitive dye while sustaining its chemical properties is crucial for successful application of this technology to live biological samples. Through the *in vitro* experiments on phantoms, a calibration curve was generated, which further enabled successful pH sensing *in vivo* on a rat joint model, with a precision better than 0.1 pH units. The nanoprobe based PAI method enables safe imaging, using only light and ultrasound, together with biocompatible, hydrogel based, biodegradable and bio-eliminable nanoparticle sensors. This resultant non-invasive and non-ionizing PAI will enable functional evaluation, across the tumors or any diseased tissues, with both high spatial and high temporal resolution, but without any damage to the tissues.

Supplementary Material

Refer to Web version on PubMed Central for supplementary material.

Acknowledgments

The authors would like to acknowledge NIH grant R21CA160157, R01AR060350 and R01AR055179, NSFC grant 11028408, and SPIE student scholarship for funding the research.

Notes and references

1. Zhang X, Lin Y, Gillies RJ. J Nucl Med. 2010; 51(8):1167–1170. [PubMed: 20660380]
2. Trédan O, Galmarini CM, Patel K, Tannock IF. J Natl Cancer Inst. 2007; 99:1441–1454. [PubMed: 17895480]
3. Andersson SE, Lexmüller K, Johansson A, Ekström GM. J Rheumatol. 1999; 26(9):2018–2024. [PubMed: 10493685]
4. Schneider LA, Korber A, Grabbe S, Dissemond J. Arch Dermatol Res. 2007; 298(9):413–420. [PubMed: 17091276]
5. Vāvere AL, Biddlecombe GB, Spees WM, Garbow JR, Wijesinghe D, Andreev OA, Engelman DM, Reshetnyak YK, Lewis JS. Cancer Res. 2009; 69(10):4510–4516. [PubMed: 19417132]
6. Gallagher FA, Kettunen MI, Day SE, Hu DE, Ardenkjær-Larsen JH, Zandt R, Jensen PR, Karlsson M, Golman K, Lerche MH, Brindle KM. Nature. 2008; 453:940–943. [PubMed: 18509335]
7. Helmlinger G, Yuan F, Dellian M, Jain RK. Nat Med. 1997; 3:177–182. [PubMed: 9018236]
8. Ray A, Koo Lee YE, Kim G, Kopelman R. Small. 2012; 8(14):2213–2221. [PubMed: 22517569]
9. Hille C, Berg M, Bressel L, Munzke D, Primus P, Löhmannsröben HG, Dosche C. Anal Bioanal Chem. 2008; 391:1871–1879. [PubMed: 18481048]
10. Xu M, Wang LV. Photoacoustic imaging in biomedicine. Rev Sci Instrum. 2006; 77:041101.
11. Ray A, Raijan J, Koo Lee YE, Wang X, Kopelman R. J Biomed Opt. 2012; 17(5):057004. [PubMed: 22612143]
12. Hovrath TD, Kim G, Kopelman R, Ashkenazi S. Analyst. 2008; 133:747–749. [PubMed: 18493674]
13. Schlageter B. Sens Actuators, B. 1997; 38–39(3):443–447.
14. Chatni MR, Yao J, Danielli A, Favazza CP, Maslov KI, Wang LV. J Biomed Opt. 2011; 16(10): 100503. [PubMed: 22029342]
15. Egginton, S.; Taylor, EW.; Raven, JA. Regulation of Tissue pH in Plants and Animals. Cambridge University Press; 1999.

16. Ray A, Wang X, Koo Lee YE, Hah HJ, Kim G, Chen T, Orringer DA, Sagher O, Liu X, Kopelman R. Nano Res. 2011; 4(11):1163–1173.
17. Guryev O, Abrams B, Lomas C, Nasraty Q, Park E, Dubrovsky T. Anal Chem. 2011; 83(18):7109–7114. [PubMed: 21846137]
18. Ray A, Koo Lee YE, Epstein T, Kim G, Kopelman R. Analyst. 2011; 136:3616–3622. [PubMed: 21773602]
19. Cheong WF, Prahl SA, Welch AJ. IEEE J Quantum Electron. 1990; 26:2166–2185.

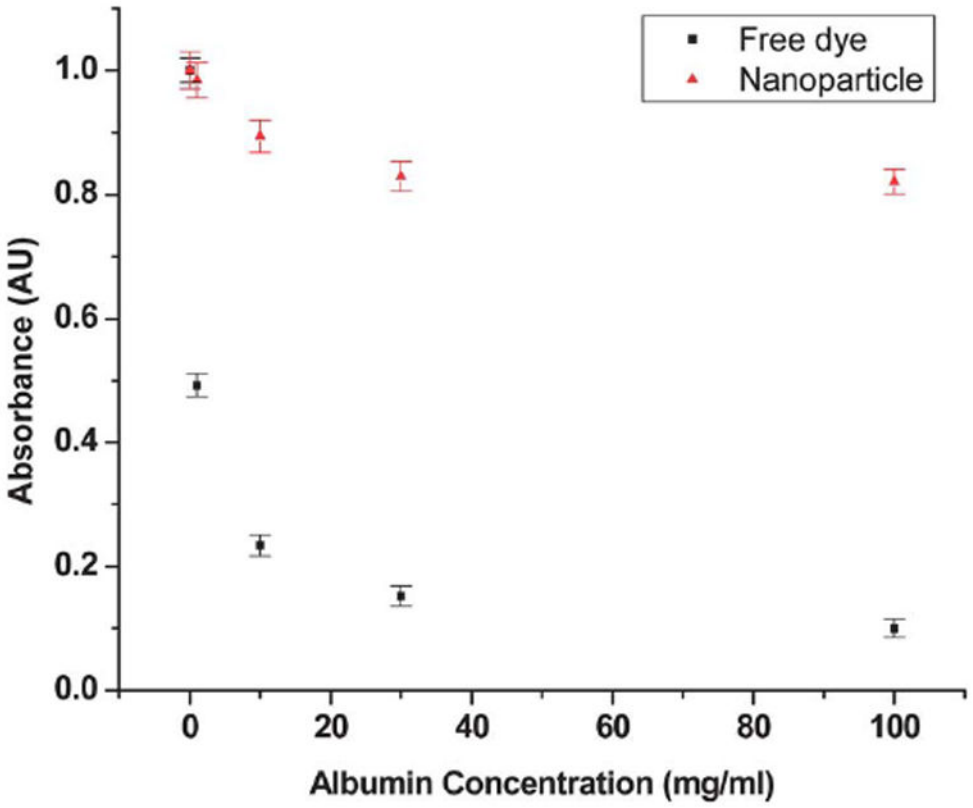

Fig. 1.

Interference with albumin. Changes in the absorption of the dye and the nanoprobe in presence of albumin. The peak absorbance at 570 nm was used to quantify the changes resulting from interaction with the proteins.

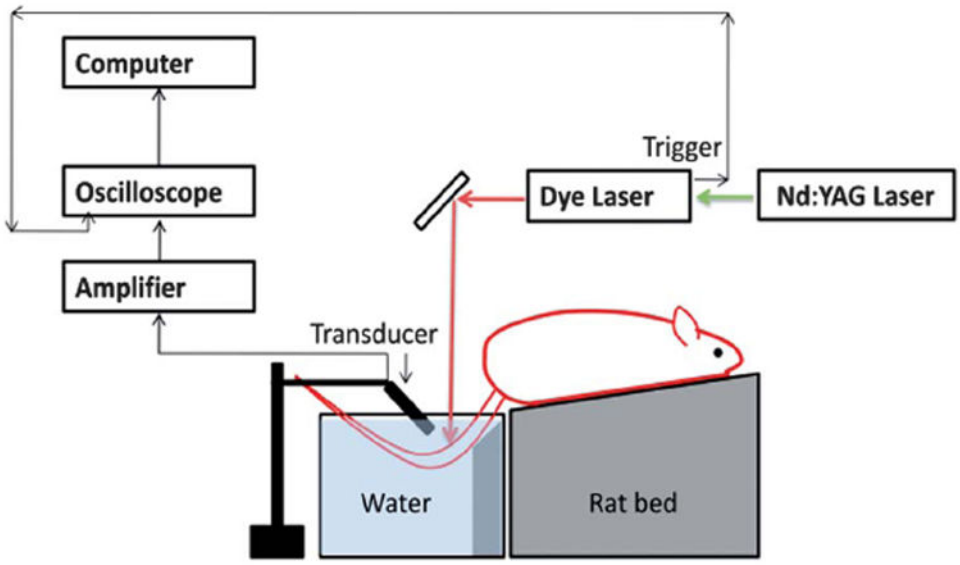

Fig. 2.
Schematic setup for the experiment on live rats.

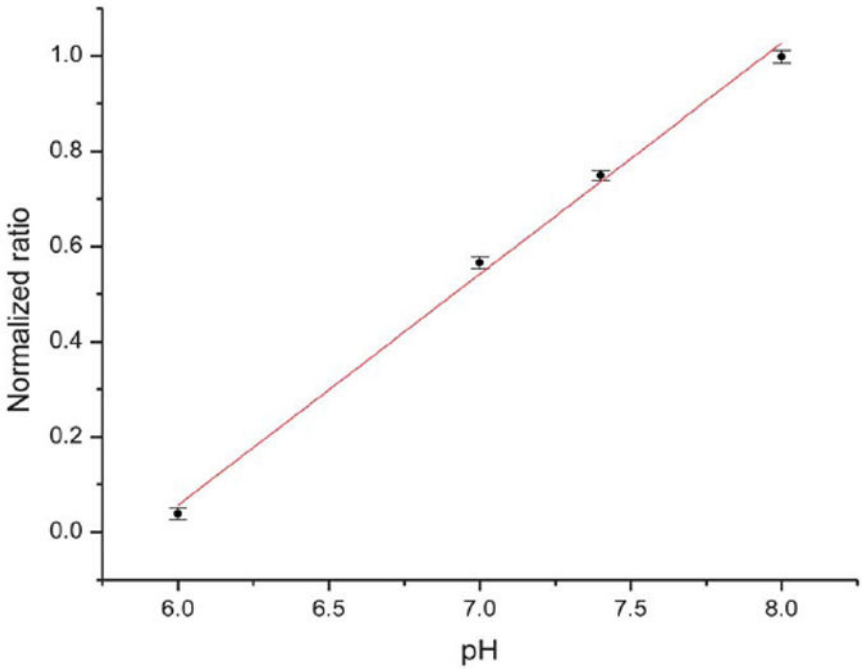

Fig. 3.

In vitro pH calibration curve. The calibration curve was obtained by taking the ratio of the photoacoustic signal intensities when the nanoprobes were illuminated at 580 nm and 565 nm, respectively.

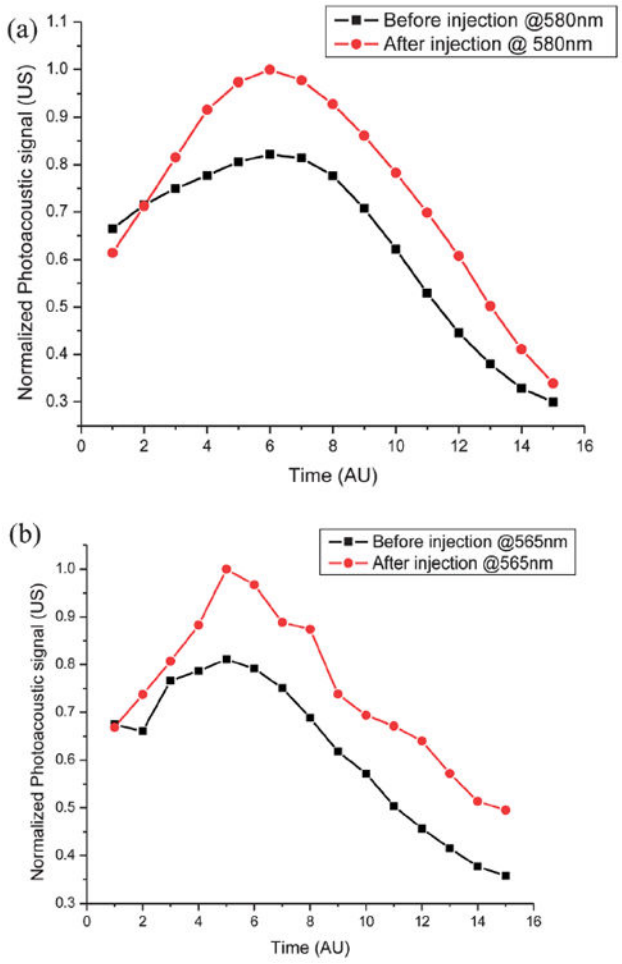

Fig. 4.

Photoacoustic signals at (a) 580 nm and (b) 565 nm, respectively, from a rat tail joint, before and after the local injection of the pH sensitive nanoprobes.